International Journal of Mass Spectrometry 306 (2011) 204–209

Contents lists available at ScienceDirect

International Journal of Mass Spectrometry

journal homepage: www.elsevier.com/locate/ijms

Interaction of small hydrocarbon ions and Ar^+ with carbon-fibre-composite surfaces at room temperature

Alan Keim [a], Bilal Rasul [a,1], Nikolaus Endstrasser [a], Paul Scheier [a], Tilmann D. Märk [a], Zdenek Herman [a,b,*]

[a] Institut für Ionenphysik und Angewandte Physik, Leopold-Franzens Universität Innsbruck, Technikerstr. 25, 6020 Innsbruck, Austria
[b] V. Čermák Laboratory, J. Heyrovský Institute of Physical Chemistry, Academy of Sciences of the Czech Republic, Dolejškova 3, 18223 Prague 8, Czech Republic

ARTICLE INFO

Article history:
Received 3 August 2010
Received in revised form 1 November 2010
Accepted 1 November 2010
Available online 9 November 2010

Keywords:
Ion-surface collisions
Ar^+ and hydrocarbon ions
Carbon-fibre-composite surface
Hydrocarbon surface coverage
Surface-induced dissociation
Surface reactions
Surface sputtering

ABSTRACT

Surface-induced interactions of projectile ions CD_3^+, $C_2D_2^+$, $C_2D_4^+$, $C_2D_5^+$, $C_2D_6^+$, and Ar^+ with room-temperature (hydrocarbon-covered) surfaces of carbon-fibre-composite (CFC) were investigated over the incident energy range of the projectile ions from a few eV up to about 100 eV. Mass spectra of the product ions and their dependence on the incident energy of the projectiles were obtained. The results showed that the extent of fragmentation of the incident molecular ions and their chemical reactions at surfaces (in case of radical cations) were similar to the interactions of these ions with room-temperature carbon (HOPG) surfaces and indicate that the hydrocarbon coverage of the surfaces primarily determines both the energy transfer at surface and its chemical reactivity. The only substantial difference was that the present mass spectra contained a certain amount of sputtered alkali ions K^+ and Na^+, most probably contaminants of the CFC material from the process of their production. Mass spectra obtained with the projectile ion Ar^+ contained sputtered ions from the surface material, namely alkali ions K^+ and Na^+ and the usual ions characterizing sputtering of surface hydrocarbons.

1. Introduction

Efficient operation of fusion devices requires the use of plasma facing materials of the first wall compatible with the operating conditions of reactor grade plasmas. Understanding interaction of ions with the material of the first wall is one of the challenges of the present fusion research. Information on surface processes of hydrocarbons and other ions, most likely vacuum contaminants in plasma devices, are essential as atomic and molecular data for modelling predictions of the ITER (International Thermonuclear Experimental Reactor) system. These data should include interaction with a variety of surfaces of materials that could be suitable materials for fusion vessels.

In our earlier work we studied interaction of hydrocarbon ions C1–C3, C6, C7, and some other non-hydrocarbon ions with room-temperature (and in some cases heated) surfaces of carbon [1–5], tokamak tiles [6], tungsten [7], beryllium [8] and, for comparison, stainless steel [9–13] and various types of diamond [14]. Surface-induced dissociation of the projectile ions in inelastic collisions with surfaces, chemical reactions at surfaces, and sputtering of surface material was observed. Information on energy partitioning in surface collisions [15,16] could be derived. Data on survival probabilities of ions colliding with room temperature and heated surfaces of the above materials were obtained [1,2,4,7] and correlations between the survival probability and ionization energy of the projectile ions on different surfaces were derived [7,8].

The results showed that at room temperature the studied surfaces were covered with a layer of hydrocarbons that determines many basic properties of the ion-surface interactions (extent of fragmentation, chemical reactions at surfaces) and the quality of the underlying surface is reflected in smaller or larger deviation from these characteristics (extent of fragmentation, inelastic energy losses, survival probabilities).

The role of hydrocarbon coverage of room-temperature surfaces is of importance in plasma and fusion devices and considerable effort has been directed to its investigation to control the impurity level of the fusion plasmas caused by erosion of the first wall. The growth of hydrocarbon C:H films by deposition of different neutral hydrocarbon species and properties of these films have been investigated [17]. The presence of hydrocarbons can be detected by sputtering or by observation of chemical reactions of some hydrocarbon ions at surfaces [18].

One of the surfaces of interest for possible use in fusion research is the surface of carbon-fibre-composite (CFC). In this communication we describe results obtained in our study of the interaction of selected C1 (CD_3^+), C2 ($C_2D_2^+$, $C_2D_4^+$, $C_2D_5^+$, $C_2D_6^+$) and some non-

---

* Corresponding author at: V. Čermák Laboratory, J. Heyrovský Institute of Physical Chemistry, Academy of Sciences of the Czech Republic, Dolejškova 3, 18223 Prague 8, Czech Republic. Tel.: +420 2 6605 3514; fax: +420 2 8658 2307.
E-mail address: zdenek.herman@jh-inst.cas.cz (Z. Herman).

[1] Present address: Department of Physics, University of Sargodha, 40100 Sargodha, Pakistan.

1387-3806/$ – see front matter © 2010 Elsevier B.V. All rights reserved.
doi:10.1016/j.ijms.2010.11.002

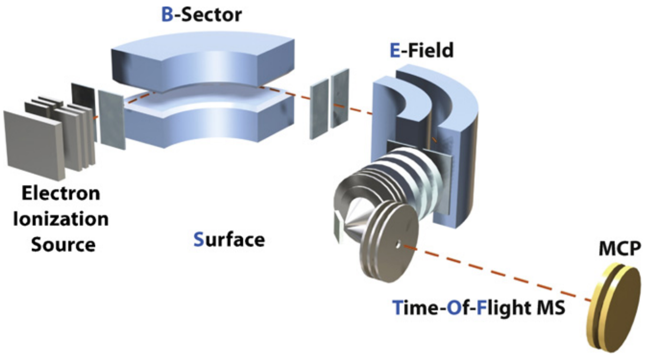

Fig. 1. Schematics of the tandem mass spectrometer BESTOF (details see text).

hydrocarbon (Ar^+) ions with this surface held at room temperature. The aim was to find similarities or differences in the ion-surface behaviour of the CFC surface in comparison with other (carbon) surfaces.

2. Experimental

2.1. Apparatus

The experiments were carried out with the tandem mass spectrometer BESTOF described in detail in our earlier papers [19,20]. In brief, the instrument consists of a double-focusing two-sector-field mass spectrometer (reversed geometry, Varian MAT CH5-DF) combined with a linear time-of-flight mass spectrometer (Fig. 1). Projectile ions were produced in a Nier-type ion source (the original commercial mass spectrometer source) by electron ionization (75 eV energy) on molecules of the gas under study. The ions produced were extracted from the ion source region and accelerated to 3 keV for mass and energy analysis by the double-focusing two-sector-field mass spectrometer. After passing the mass spectrometer exit slit, the ions were refocused by an Einzel lens and decelerated to the required incident energy, before interacting with the target surface. Shielding the target area with conical shield lenses minimized field penetration effects. The incident impact angle of the projectile beam was kept at 45° and the scattering angle was fixed at 46° (with respect to the surface). The incident energy of ions impacting on the surface was defined by the potential difference between the ion source and the surface. The energy spread of the primary ion beam was determined by measuring the (reflected) ion signal as a function of the increasing positive surface potential in the same geometry. The energy spread of the primary beam of the projectile ions was in the range of 250 to 300 meV (full-width at half-maximum). A fraction of the product ions formed at the surface exited the shielded chamber through a 1 mm diameter orifice. The ions were then subjected to a pulsed deflection-and-acceleration field that initiated the time-of-flight analysis of the ions. The second mass analyzer was thus a linear time-of-flight (TOF) mass selector with a flight tube of about 80 cm length. The mass selected ions were detected by a double-stage multi-channel plate connected to a multi-channel scaler (time resolution of 10 ns per channel) and a computer. The product ion intensities were obtained by integration of the recorded signals. The pressure in the ion source was $2–6 \times 10^{-6}$ Torr, the bakeable surface chamber and the TOF analyzer were maintained under ultra-high vacuum conditions (10^{-9} Torr) by a turbo-pump. However, even these ultra-high vacuum conditions did not exclude deposition of a layer of hydrocarbons on the surface, whenever the valve between the sector field mass spectrometer and the surface chamber was opened and the pressure in the surface region increased to the 10^{-8} Torr range.

Mass spectra of the product ions from collisions of the projectile ions with the CFC surfaces kept at room temperature were recorded at a series of incident energies and relative abundances of the product ions were plotted as a function of the projectile ion energy (energy-resolved-mass-spectra, ERMS curves).

2.2. CFC surface

The carbon-fibre-composite used was of the type NB-31, obtained from the Max-Planck Institute of Plasma Physics in Garching. The samples of this carbon-fibre-composite material were kept during the experiments at room temperature. Under these conditions, the surfaces were covered with a layer of background hydrocarbons, despite a surface chamber vacuum of the order of 2×10^{-9} Torr. The occurrence of H-atom transfer reactions between radical projectile ions ($C_2D_4^+$ etc.) and terminal H-atoms of the hydrocarbons on the surface [1–3,7,8,16] is a strong evidence for this surface coverage.

3. Results and discussion

3.1. Ar^+

Mass spectra of product ions from collisions of Ar^+ (energies up to 100 eV) with the CFC surface at room temperature (Fig. 2, left) may contain ions from sputtering of the surface material and from the chemical reaction of H-atom transfer with the surface hydrogen

$$Ar^+ + CH_3–S \rightarrow ArH^+ + {}^{\bullet}CH_2–S \quad (1)$$

Assuming an average bond strength of $H–CH_2$— in the terminal group of surface aliphatic hydrocarbons of 2.1 ± 0.3 eV [1] reaction (1) is exothermic by about 1.6 eV and may occur. However, the intensity of m/z 41 in the spectra does not exceed considerably the intensities of ions at m/z 42 and 43 that should result from sputtering of surface hydrocarbons. The ratio of intensities at m/z 41/43 is 1.5–1.7 for collisions of Ar^+ of incident energies of 30–100 eV with room-temperature CFC (see Fig. 2) and this ratio is similar to the ratio of intensities at m/z 41/43 from collisions of CD_3^+ with room-temperature CFC (see also Fig. 3 later on), 1.6 (at 30 eV) and 3.0 (at 75 eV), where no reaction analogous to reaction (1) can occur and the contribution of carbon chain build-up reactions leading to C3 ions is negligible [1]. Therefore, it appears that reaction (1) does not contribute significantly to the intensity of the ion of m/z 41 and product ions at m/z 40–43 result from sputtering of the surface hydrocarbons.

Product ions at m/z 23 (Na^+) and m/z 39 (K^+) indicate the presence of alkali ions. However, the intensity at m/z 39 is likely to contain contributions from both sputtered K^+ and sputtered hydrocarbon ion $C_3H_3^+$. Contribution of the sputtered hydrocarbon ion may be estimated from experiments on Ar^+ collisions with other surfaces in which no alkali ions were detected. From studies of Ar^+ collisions (incident energy 30–100 eV) with room-temperature (hydrocarbon-covered) plasma-sprayed tungsten surfaces [21] and O-terminated diamond surface [14] it follows that the ratio of sputtered ion intensities $I(C_3H_3^+)/I(C_3H_5^+)$ (m/z 39/43) is 0.6–1.0. If we correct the intensity of m/z 39 by subtracting this contribution of the intensity at m/z 43, the remaining intensity at m/z 39 should be that of K^+. This intensity is then slightly larger than the intensity of sputtered Na^+ (m/z 23). The data are summarized in Fig. 2, left

The remaining product ion in the mass spectra from Ar^+-CFC collisions are sputtered hydrocarbon ions at m/z 27 ($C_2H_3^+$) and 29 ($C_2H_5^+$), 41 ($C_3H_5^+$) and 43 ($C_3H_7^+$), 55 ($C_4H_7^+$) and 57 ($C_4H_9^+$), and at higher incident energies small amount of ions at m/z 67 ($C_5H_7^+$), 69 ($C_5H_9^+$) and 71 ($C_5H_{11}^+$). These closed-shell cations are typical for sputtering of surfaces covered with alkanes, indicating that

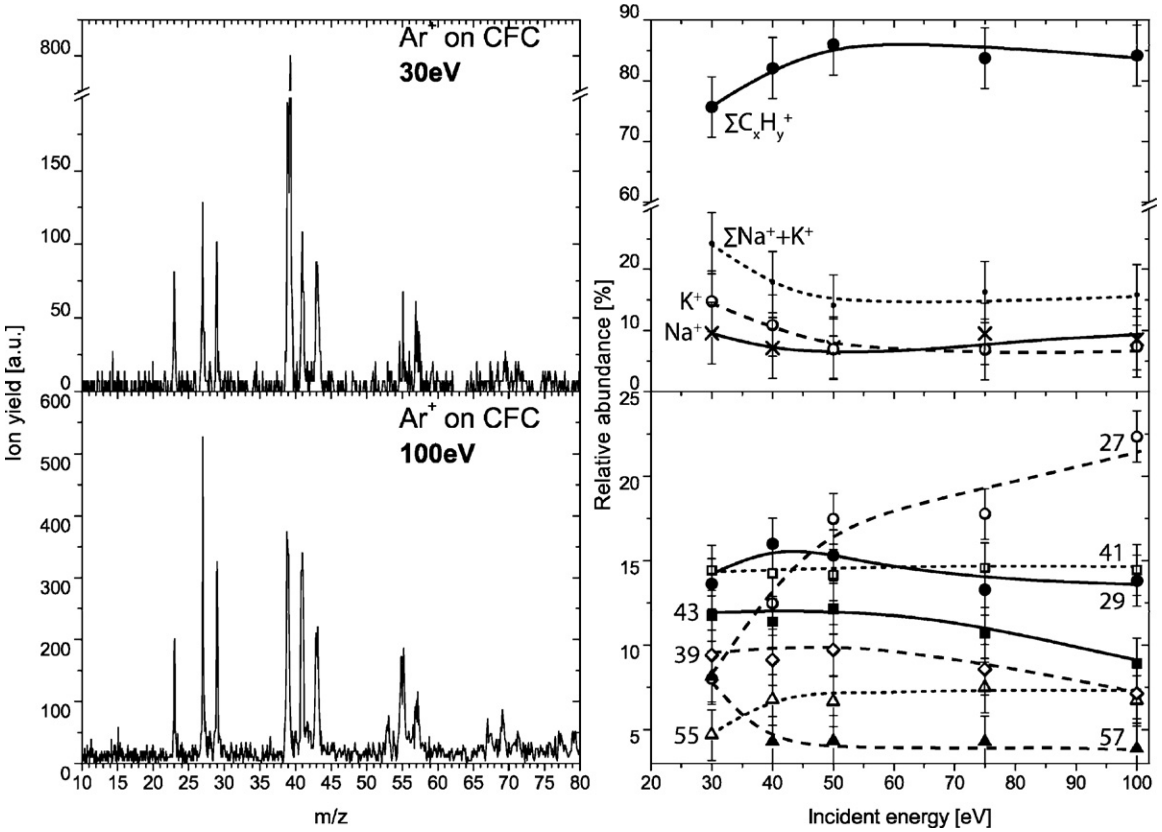

Fig. 2. Product ions from collisions of Ar^+ with room temperature CFC surface. Left: mass spectra at the incident energy of Ar^+ of 30 eV and 100 eV. Upper right: relative abundance of the sum of all sputtered hydrocabon ions, the sum of the abundance of both alkali ions, $K^+ + Na^+$ (dashed line), and the K^+ and Na^+ abundance as a function of incident energy of Ar^+. Lower right: relative abundance of different hydrocarbon ions as a function of the incident energy of Ar^+ (alkali ions not shown).

the CFC surface was covered at room temperature with a layer of background hydrocarbons.

The spectra show measurable amounts of sputtered ions only at incident energies above about 20 eV. Fig. 2 (upper right) gives the relative amount of K^+, Na^+, and the sum of hydrocarbon ions as a function of the incident energy (ERMS curves of product ions). The relative amounts of these sputtered components do not change significantly over the incident energy range 30–100 eV: the relative abundance of all hydrocarbon ions increases from about 75% to 85%, while the relative amount of the sputtered alkali ions decreases from about 15% to 10% and their ratio K^+/Na^+ is 1.2 ± 0.15.

Fig. 2 (lower right) provides then the ERMS curves for the individual sputtered hydrocarbon ions (normalized to the total intensity of all ions, both hydrocarbon and alkali ions). A small decrease of m/z 29 vs. 27, 43 vs. 41, and 57 vs. 55 indicates that part of the sputtered ions further dissociates. The ERMS curves in Fig. 2 show only the relative abundances of the product ions, their absolute intensities decrease with decreasing incident energy and below about 20 eV no measurable amounts of sputtered ions could be observed.

3.2. CD_3^+

Mass spectra from collisions of CD_3^+ with the room temperature CFC surface (examples see Fig. 3) show even at large incident energy a considerable contamination by projectile ions CD_3^+ deflected by surface charges. This can be well seen in comparison with earlier obtained spectra on this machine [10] in collisions of CH_3^+ with room temperature stainless steel surface or spectra from collisions of CD_3^+ with room temperature carbon (HOPG) surface [1]. Besides

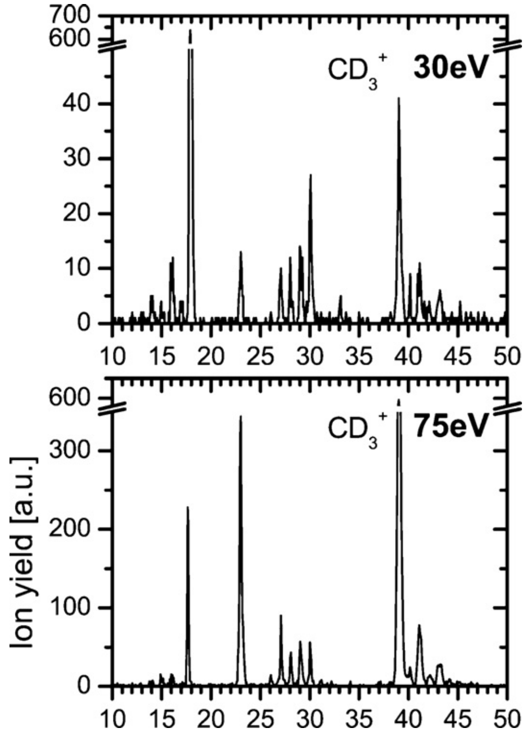

Fig. 3. Mass spectra of product ions from collisions of CD_3^+ of incident energiy 30 eV and 75 eV with a room-temperature CFC surface.

that, the spectra show other phenomena observed in the above mentioned previous studies, namely

(i) Collision-induced dissociation of the projectile ion to give fragment ions CD_2^+ (*m*/*z* 16) and CD^+(*m*/*z* 14) in reactions

$$CD_3{}^+ + S \rightarrow CD_2{}^+ + D \tag{2}$$

$$CD_3{}^+ + S \rightarrow CD^+ + D_2 \tag{3}$$

It has been shown in previous studies that the product ions of dissociation reactions have similar velocity distributions as the inelastically scattered undissociated projectile ion, indicating that the dissociation occurs after the interaction with the surfaces as a unimolecular process.

(ii) A chemical reaction of H-atom transfer with surface hydrocarbons

$$CD_3{}^+ + CH_3\text{–}S \rightarrow CD_3H^+ + {}^\bullet CH_2\text{–}S \tag{4}$$

is endothermic by about 2.5 eV and most probably does not take place (no trace of CD_3H^+ was observed). A very small contribution of ions of odd masses *m*/*z* 17 (CD_2H^+) and its fragments (of which CDH^+ can be observed at *m*/*z* 15) presumably come from an exchange reaction with H-atoms of the surface

(iii) Sputtering of the surface material giving rise, similarly as in Ar^+ collisions, to contributions of sputtered alkali ions at *m*/*z* 23 (Na^+) and *m*/*z* 39 (K^+), and sputtered hydrocarbon ions at *m*/*z* 27, 29, 39, 41, and 43; a correction of *m*/*z* 39 for the contribution of sputtered $C_3H_3^+$ (see above) does not change the intensity of *m*/*z* 39 significantly.

(iv) A small contribution of chemical carbon chain build-up reactions between the projectile ion and terminal groups of hydrocarbons on the surface, leading to partially deuterated ions $C_2X_3^+$, $C_2X_4^+$, and $C_3X_3^+$ (X = H,D) that overlap with the sputtered hydrocarbon ions as mentioned in (iii). A detailed discussion of these reactions has been given in Ref. [1] on the basis of data from collisions of CH_3^+, $^{13}CH_3^+$, and CD_3^+ with a room-temperature carbon surface. The previously suggested mechanism of C2 product ion formation [1] assumed a reaction between CD_3^+ and terminal CH_3-group of surface hydrocarbons

$$CD_3{}^+ + CH_3\text{–}CH_2\text{–}S \rightarrow CH_2D\text{–}S + [CD_2\text{–}CH_3{}^+] \rightarrow C_2X_3{}^+ + X_2 \tag{5}$$

with X = H,D. However, the presence of *m*/*z* 30 and 33 in the mass spectra from CD_3^+-CFC collisions indicates another possible mechanism, namely

$$CD_3{}^+ + CH_3\text{–}CH_2\text{–}S \rightarrow {}^\bullet CH_2\text{–}S + [CD_3\text{–}CH_3{}^{+\bullet}] \rightarrow C_2X_4{}^{+\bullet} + X_2 \tag{6}$$

The most important difference between collisions with the room-temperature (hydrocarbon-covered) CFC surface and the room-temperature carbon (HOPG) surface concerns the sputtering of alkali metal ions, that was not observed on the carbon (HOPG) surface. The sputtering of alkali ions increases with increasing incident energy of CD_3^+ from 4% of all product ions at 20 eV to 80% of all product ions at 100 eV. The relative amount of K^+ vs. Na^+ shows a decrease over this collision energy range, too, from a value for the ratio of 2.5 at 30 eV to about 1.7 at 100 eV. While at low collision energies fragmentation and chemical reactions of the projectile ion represent a substantial part of the product ions, above 75 eV sputtering and formation of alkali metal ions dominates.

3.3. $C_2D_2^+$, $C_2D_4^+$, $C_2D_5^+$, $C_2D_6^+$

Mass spectra of product ions from collisions of projectile ions $C_2D_2^+$, $C_2D_4^+$, $C_2D_5^+$, $C_2D_6^+$ with the room temperature (hydrocarbon-covered) CFC surfaces show basically similar product ions that were observed in collisions of these ions with room temperature (hydrocarbon-covered) surfaces of carbon (HOPG) [2,5] or even tungsten [7] or stainless steel [14] (data for $C_2D_4^+$ only). In general, there is a difference between the interaction of radical cations (like $C_2D_2^+$, $C_2D_4^+$, $C_2D_6^+$) and closed-shell ions (like $C_2D_5^+$). While the closed-shell ions exhibit only surface-induced dissociations of the projectile ions and sputtering of the surface material, the radical cations show in addition chemical reactions of H-atom transfer and carbon chain build-up with surface hydrocarbons (formation of C3 ions). Data in Fig. 4 give, as an example, mass spectra of ion products from collisions of $C_2D_2^+$, $C_2D_4^+$, $C_2D_5^+$, and $C_2D_6^+$ at the incident energy of 30 eV.

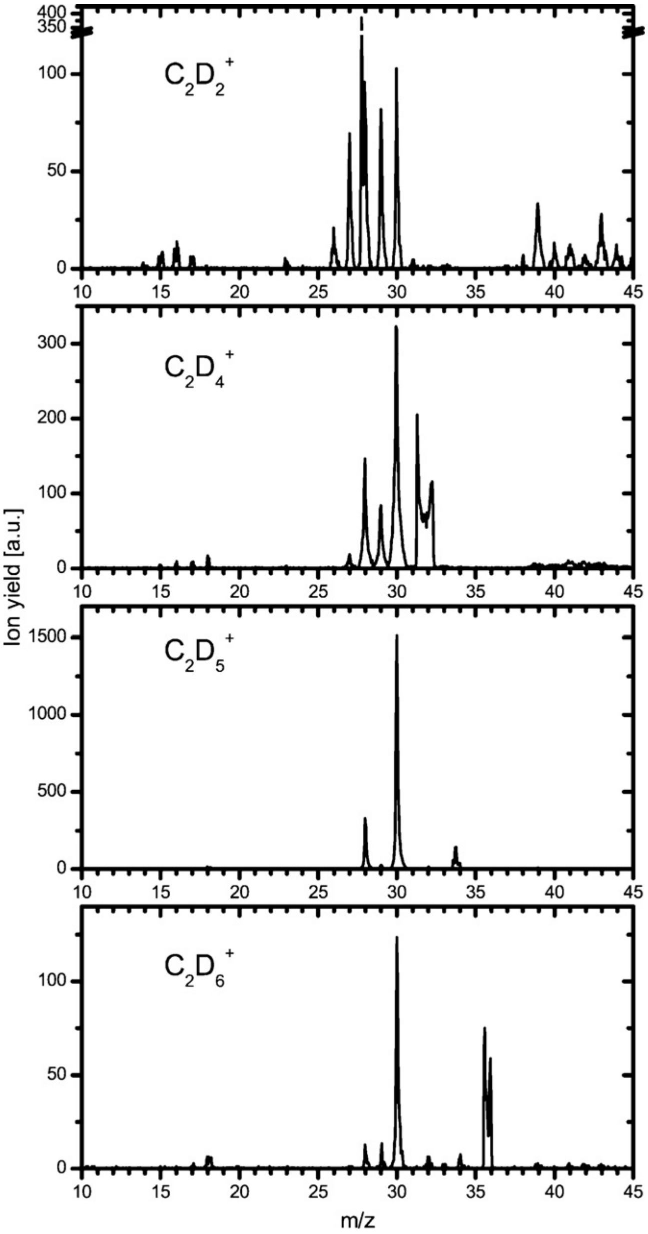

Fig. 4. Mass spectra of product ions from collisions of $C_2D_2^+$, $C_2D_4^+$, $C_2D_5^+$, and $C_2D_6^+$ with a room-temperature CFC surface at the incident energy of the projectile ions of 30 eV.

The mass spectrum of products from $C_2D_5^+$ collisions indicates only fragmentation of the incident ion (*m*/*z* 34, almost fully fragmented) to the product ions at *m*/*z* 30 ($C_2D_3^+$) and 28 ($C_2D_2^+$). The closed-shell $C_2D_5^+$ has a higher survival probability than the

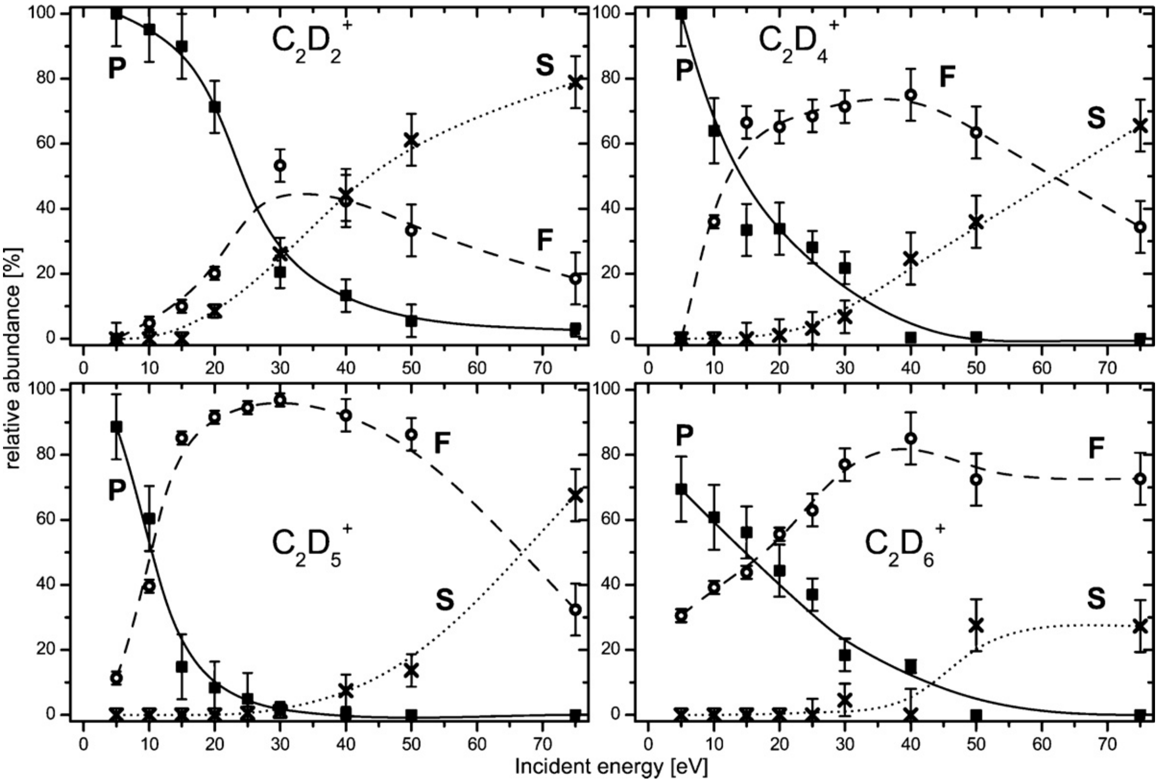

Fig. 5. ERMS curves of product ions from collisions of $C_2D_2^+$, $C_2D_4^+$, $C_2D_5^+$, and $C_2D_6^+$ with a room-temperature CFC surface. P – inelastically scattered undissociated projectile ions (full squares, full line), F – sum of all fragment ions (open points, dashed), S – sum of all sputtered ions (crosses, dotted).

other C2 ions under investigation (about 1% with respect to 0.1% for $C_2D_2^+$) and the sputtering processes are seemingly suppressed in the scale of Fig. 4 ($C_2D_5^+$).

Mass spectra of product ions from collisions of $C_2D_2^+$, $C_2D_4^+$, and $C_2D_6^+$ show both fragmentation products at even masses below the almost fully fragmented molecular ion and products of reactions of H-atom transfer with the hydrocarbon on the surface (fragment ions at odd *m*/*z*, and the respective statistical contributions at the relevant even masses). The reactivity of $C_2D_6^+$ for H-atom transfer appears to be much lower than the reactivity of $C_2D_2^+$ and $C_2D_4^+$. The peak at the incident ion mass shows in all cases a split structure: the peak of ion intensity shifted by a fraction of *m*/*z* to a lower mass is due to fast ions of full incident energy, deflected in front of the surface by surface charges without making a surface collision (see Section 2.2) and was not taken into consideration in evaluating the product of surface interactions. Formation of C3 products [2] in reactions of the projectile radical cation with the terminal CH_3–groups of the surface hydrocarbons seems to play a minor role at this incident energy.

The data on product ions from collisions of the C2 hydrocarbon ions with the CFC surface as a function of incident energy are summarized as ERMS curves in Fig. 5. The ERMS curves show the relative abundance of inelastically scattered undissociated projectile ions, the sum of all fragment ions (both direct fragmentations and products of chemical reactions with surface and their fragmentation), and product ions from sputtering of the surface material. The fraction of sputtered ions, barely observable at the incident energy of 30 eV, increased significantly with the incident energy. The sputtered ions are the usual hydrocarbon ions (see Section 3.1) and the alkali metal ions Na^+ and K^+. At 75 eV the alkali ions represented 60–70% of all product ions in case of $C_2D_2^+$, $C_2D_4^+$, and $C_2D_5^+$, similarly as in collisions of CD_3^+. In collisions with $C_2D_6^+$ the fraction of alkali ions was only about 30%.

4. Conclusions

The mass spectra of product ions from collisions of the CD_3^+, $C_2D_2^+$, $C_2D_4^+$, $C_2D_5^+$, $C_2D_6^+$ hydrocarbon ions with the carbon-fibre-composite (CFC) surface kept at room temperature (hydrocarbon-covered) show a similar extent of fragmentation and similar chemical reactivity with the surface as these ions exhibited with a room-temperature carbon (HOPG) surface and, for that matter, all hydrocarbon-covered surfaces so far studied by us (stainless steel, tungsten, and diamond). This finding indicates that the energy transfer and chemical reactivity of these surfaces is basically determined by the hydrocarbon surface coverage, in agreement with many previous findings [1–4,7,14,22].

The only substantial difference is in the sputtering of the surface material that shows the presence of alkali metal contaminants (presence of Na^+, K^+ ions) originating presumably from the process of preparation of CFC surfaces of this type.

The results from collisions of Ar^+ with the room temperature CFC surface are in agreement with these findings. These collisions lead mostly to sputtering of the surface material and show the presence of both alkali ions Na^+ and K^+ and the typical hydrocarbon ions sputtered from hydrocarbon-covered surfaces.

Acknowledgments

We dedicate this paper to Professor Tino Gäumann on the occasion of his 85th birthday as an expression of many decades of respect to his personality and to his contribution to the field of mass spectrometry.

This work, supported by the European Communities under the Contracts of Association between EURATOM ÖAW and EURATOM IPP.CR, was carried out within the framework of the European Fusion Development Agreement (EFDA). The views and opinions expressed herein do not necessarily reflect those of the European Commission. The research was partly supported by FWF, Wien.

References

[1] J. Roithová, J. Žabka, Z. Dolejšek, Z. Herman, J. Phys. Chem. B 106 (2002) 8293.
[2] J. Jašík, J. Žabka, L. Feketeová, I. Ipolyi, T.D. Märk, Z. Herman, J. Phys. Chem. A 109 (2005) 10208.
[3] A. Pysanenko, J. Žabka, F. Zappa, T.D. Märk, Z. Herman, Int. J. Mass Spectrom. 273 (2008) 35.
[4] A. Pysanenko, J. Žabka, L. Feketeová, T.D. Märk, Z. Herman, Eur. J. Mass Spectrom. 14 (2008) 335.
[5] A. Pysanenko, J. Žabka, Z. Herman, Collect. Czech. Chem. Commun. 73 (2008) 755.
[6] J. Žabka, Z. Dolejšek, J. Roithová, V. Grill, T.D. Märk, Z. Herman, Int. J. Mass Spectrom. 213 (2002) 145.
[7] A. Pysanenko, J. Žabka, T.D. Märk, Z. Herman, Int. J. Mass Spectrom. 277 (2008) 229.
[8] Z. Herman, J. Žabka, A. Pysanenko, J. Phys. Chem. A 113 (2009) 14838.
[9] R. Wörgötter, J. Kubišta, J. Žabka, Z. Dolejšek, T.D. Märk, Z. Herman, Int. J. Mass Spectrom. Ion Process. 174 (1998) 53.
[10] A. Qayyum, T. Tepnual, C. Mair, S. Matt-Leubner, P. Scheier, Z. Herman, T.D. Märk, Chem. Phys. Lett. 376 (2003) 539.
[11] A. Qayyum, Z. Herman, T. Tepnual, C. Mair, S. Matt-Leubner, P. Scheier, T.D. Märk, J. Phys. Chem. A 108 (2004) 1.
[12] L. Feketeová, T. Tepnual, V. Grill, P. Scheier, J. Roithová, Z. Herman, T.D. Märk, Int. J. Mass Spectrom. 265 (2007) 337.
[13] L. Feketeová, V. Grill, F. Zappa, N. Endstrasser, B. Rasul, Z. Herman, P. Scheier, T.D. Märk, Int. J. Mass Spectrom. 276 (2008) 37.
[14] L. Feketeová, J. Žabka, F. Zappa, V. Grill, P. Scheier, T.D. Märk, Z. Herman, J. Am. Soc. Mass Spectrom. 20 (2009) 927.
[15] J. Kubišta, Z. Dolejšek, Z. Herman, Eur. Mass Spectrom. 4 (1998) 311.
[16] Z. Herman, J. Am. Soc. Mass Spectrom. 14 (2003) 1360.
[17] C. Hopf, K. Letourneur, W. Jacob, T. Schwarz-Selinger, A. von Keudell, Appl. Phys. Lett. 74 (1999) 3800.
[18] Z. Herman, EFDA Newsl. 3 (2005) 7.
[19] C. Mair, T. Fiegele, F. Biasioli, R. Wörgötter, V. Grill, M. Lezius, T.D. Märk, Plasma Source Sci. Technol. 8 (1999) 191.
[20] C. Mair, T. Fiegele, F. Biasioli, Z. Herman, T.D. Märk, J. Chem. Phys. 111 (1999) 2770.
[21] B. Rasul, Thesis, Leopold-Franzens Universität Innsbruck, 2009, p. 72.
[22] R.G. Cooks, T. Ast, A. Mabud, Int. J. Mass Spectrom. Ion Process. 100 (1990) 209, and references cited therein.